Results in Physics 23 (2021) 103973

Contents lists available at ScienceDirect

Results in Physics

journal homepage: www.elsevier.com/locate/rinp

W-shaped and other solitons in optical nanofibers

K.S. Al-Ghafri [a,*], E.V. Krishnan [b], Anjan Biswas [c,d,e,f]

[a] University of Technology and Applied Sciences, P.O. Box 14, Ibri 516, Oman
[b] Department of Mathematics, Sultan Qaboos University, P.O.Box 36, Al-Khod 123, Muscat, Oman
[c] Department of Physics, Chemistry and Mathematics, Alabama A&M University, Normal, AL 35762-4900, USA
[d] Mathematical Modeling and Applied Computation (MMAC) Research Group, Department of Mathematics, King Abdulaziz University, Jeddah 21589, Saudi Arabia
[e] Department of Applied Mathematics, National Research Nuclear University, 31 Kashirskoe Hwy, Moscow 115409, Russian Federation
[f] Department of Mathematics and Applied Mathematics, Sefako Makgatho Health Sciences University, Medunsa-0204, Pretoria, South Africa

ARTICLE INFO

Keywords:
W-shaped soliton
Numerous optical solitons
Nano optical fibers
Perturbed nonlinear Schrödinger equation
Modulation instability

ABSTRACT

The main objective of this study is to investigate W-shaped and other types of optical solitons in nano optical fibers. The medium is described by perturbed nonlinear Schrödinger equation with Kerr law nonlinearity. The study is carried out by means of three exotic soliton ansatzes. Consequently, different forms of W-shaped solitons are derived under specific conditions. It is found that the formation of W-shaped solitons depends on the balance between the self-steepening effect and the nonlinear dispersion. Due to some restrictions, W-shaped solitons experience a decay into bright or dark solitons. Besides, numerous types of soliton solutions that describe different structures of optical solitons are extracted. These structures include bright, dark, kink-dark, kink and anti-kink solitons. The existence conditions of all optical solitons are presented. The behaviours of optical solitons are illustrated graphically by selecting suitable values for the physical parameters.

1. Introduction

Recently, the nonlinear Schrödinger (NLS) family of equations have received remarkable attraction because their models describe different media in physical and engineering sciences such as nonlinear optics, plasma physics, fluid dynamics, quantum electronics, and Bose–Einstein condensates [1–6]. There are a lot of generalized forms of NLS equation that have been developed in physics such as Radhakrishnan–Kundu–Laskshmanan model [7], Fokas–Lenells equation [8], Kundu–Mukherjee–Naskar model [9]. Herein, we focus on one of the nonlinear dynamical problems that appear in the nano optical fibers. This field of study has been under intense attention by the experts from around the world and it is known to be characterized by a model of perturbed NLSE. For instance, Yin et al. [10] investigated the perturbed NLSE with the power-law nonlinearity in a nano optical fiber by employing the bifurcation theory and qualitative theory. Based on the equilibrium points, they derived chaotic motions for this equation. With dual-power law nonlinearity, the NLS equation in presence of Hamiltonian perturbation terms in nano optical fibers is examined by Bouzida et al. [11]. The chirped solutions consisting of bright, dark and singular solitons are generated. By means of Adomian decomposition method, Biswas et al. [12] reported on optical soliton perturbation with Kerr law nonlinearity, where bright and dark type solitons are recovered. More recently, the complex solitons of perturbed NLSE arising in nano-fibers are extracted via the generalized exponential rational function method by Gao et al. [13], where all solutions are obtained with constant phase. Sulaiman et al. [14] studied the space–time fractional perturbed NLSE in nano-fibers. By applying the extended sinh-Gordon equation expansion method, they obtained optical solitons and singular periodic wave solutions. Similarly, Nestor et al. [15] dealt with the previous model using two integration schemes. Series of optical soliton solutions with fractional derivative order are revealed.

The envelope solitons are considered as one of the powerful tools for understanding the physical phenomena in nonlinear optics, as example. They have been used as a carrier of information through optical fibers over transcontinental and transoceanic distances in a matter of a few femtoseconds. Thus, a variety of mathematical models have been studied by many researchers through applying different integration schemes to derive optical soliton solutions. The employed integration methodologies on investigating solitons include generalized G'/G-expansion method, improved $\tan(\phi(\xi)/2)$-expansion method, semi-inverse variational principle, extended trial equation method, Lie group method, improved projective Riccati equations method, modified Kudryashov's method, Weierstrass elliptic function method and many others. For more

* Corresponding author.
E-mail address: khalil.ibr@cas.edu.om (K.S. Al-Ghafri).

https://doi.org/10.1016/j.rinp.2021.103973
Received 22 December 2020; Received in revised form 2 February 2021; Accepted 8 February 2021

details, the reader is referred to references [16–32].

Solitons, in the context of photonics, are known to have different structures such as bright, dark and singular solitons. In addition to these forms of soliton pulses, there is an interesting type called W-shaped soliton. Many recent studies have been drawn toward the investigation of solitons of W-shaped type in various models of the NLS family of equations where this type of solitons may contribute on interpreting the physics of those media. For example, Li et al. [33] derived new types of solitary wave solutions for the higher order nonlinear Schrödinger equation describing propagation of femtosecond light pulses in an optical fiber. It is found that these solutions represent W-shaped solitary waves. Furthermore, Zhao et al. [34] investigated the rational solutions on a continuous-wave background in the Sasa-Satsuma equation. The study is carried out analytically by applying the Darboux transformation method. The obtained solution describes the W-shaped soliton in a nonlinear fiber with higher-order effects including higher-order dispersion, Kerr dispersion, and stimulated inelastic scattering. Moreover, Triki et al. [35] examined chirped W-shaped optical solitons of Chen-Lee-Liu equation by implementing localized soliton ansatz in term of the secant hyperbolic function plus a constant background field. Then, the former model has been studied by González-Gaxiola and Biswas [36] to retrieve W-shaped solitons using a numerical scheme, namely, Laplace Adomian decomposition method. Additionally, different types of soliton solutions for an extended nonlinear Schrödinger equation with third- and fourth-order dispersion terms for describing ultrashort pulse propagation in highly dispersive media have been extracted by the aid of three forms of a complex amplitude ansatzes in reference [37]. Among them, the solitary wave of W-shape profile is induced. Furthermore, Triki et al. [38] investigated a generalized NLS equation with higher-order effects in negative indexed materials. They found three new types of non-linearly chirped W-shaped solitons as well as bright solitons by utilizing the traveling-wave method.

The target of this work is to generalize the technique used by Triki et al. [38] to derive W-shaped solitons in nano optical fibers. Thus, a three general ansatzes are developed and applied to the perturbed NLSE with Kerr law nonlinearity. Further to W-shaped soliton, we derive different types of exact analytic solutions which construct bright, dark, kink, anti-kink and kink-dark solitons. The existence conditions for all of these types of solitons are demonstrated. The optical soliton solutions obtained here have nontrivial phases which are dependent on the pulse intensity.

This manuscript is organised as follows. In Section 2, we discuss the governing model of perturbed NLSE and we derive the traveling wave reduction for the proposed model. In Section 3, three forms of soliton ansatzes are assumed to find the exact solutions. Numerous optical pulses including W-shaped, bright, dark, kink, anti-kink and kink-dark solitons are extracted. In Section 4, the modulation instability by means of standard linear stability analysis is examined. The outlook and discussion on the results obtained are presented in Section 5. Finally, Section 6 contains our summary and conclusion.

2. Governing model and its traveling wave reduction

The model of perturbed Nonlinaer Schrödinger equation (NLSE) which is dealt with in the present study is described by [13–15]

$$iq_t + aq_{xx} + b|q|^2 q - i\left(\sigma q_x - \lambda(|q|^2 q)_x - \gamma(|q|^2)_x q\right) = 0, \tag{1}$$

where $q(x,t)$ is a complex valued function representing the wave profile in optical fibers whereas x and t are the independent variables standing for spatial and temporal coordinates. The coefficients a and b denote the group velocity dispersion and the nonlinear effect, respectively. The last three terms indicate the perturbation influences where σ is the inter-modal dispersion, λ is the self-steepening perturbation term and γ is the nonlinear dispersion coefficient.

In the absence of perturbation terms (i.e., $\sigma = \lambda = \gamma = 0$), Eq. (1) reduces to the standard NLSE which describes the propagation of pico-second optical pulse in optical fibers. However, once scrutinizing femtosecond width optical pulses, then the higher-order effects become unavoidable in the model as shown in Eq. (1). Basically, this equation provides soliton solution that arises due to a delicate balance between dispersion and nonlinearity.

In order to find the optical soliton solutions for Eq. (1), we consider the traveling wave transformation of the form

$$q(x,t) = u(\xi)e^{i(\phi(\xi)-\omega t)}, \tag{2}$$

where $\xi = x - \nu t$ is the traveling variable while ω and ν are real parameters. Both $u(\xi)$ and $\phi(\xi)$ are real functions which represent the pulse shape and nonlinear phase shift, respectively.

Substituting (2) into Eq. (1) and separating the imaginary and real components, one can find the system of equations

$$-(\nu+\sigma)u' + 2au'\phi' + au\phi'' + (3\lambda+2\gamma)u^2u' = 0, \tag{3}$$

$$au'' + \omega u + bu^3 + (\nu+\sigma)u\phi' - au\phi'^2 - \lambda u^3\phi' = 0, \tag{4}$$

where the prime denotes the derivative with respect to ξ. Upon multiplying Eq. (3) by u, one obtains the first integral in the form

$$\frac{(\nu+\sigma)}{2}u^2 - au^2\phi' - \frac{(3\lambda+2\gamma)}{4}u^4 = C, \tag{5}$$

where C is the constant of integration. Eq. (5) can be rewritten as

$$\phi' = \frac{(\nu+\sigma)}{2a} - \frac{(3\lambda+2\gamma)}{4a}u^2 - \frac{C}{a}u^{-2}. \tag{6}$$

Now, substituting Eq. (17) into Eq. (4), we find

$$u'' + A_1u + A_2u^3 + A_3u^5 - A_4u^{-3} = 0. \tag{7}$$

To simplify Eq. (7), we multiply by u' and integrate with respect to ξ to arrive at

$$u'^2 + A_1u^2 + \frac{A_2}{2}u^4 + \frac{A_3}{3}u^6 + A_4u^{-2} + 2A_0 = 0, \tag{8}$$

where A_0 is an arbitrary constant of integration and A_1, A_2, A_3, A_4 are given by

$$A_1 = \frac{2a\omega + (\nu+\sigma)^2 - C(\lambda+2\gamma)}{2a^2}, \tag{9}$$

$$A_2 = \frac{2ab - \lambda(\nu+\sigma)}{2a^2}, \tag{10}$$

$$A_3 = \frac{3\lambda^2 - 4\lambda\gamma - 4\gamma^2}{16a^2}, \tag{11}$$

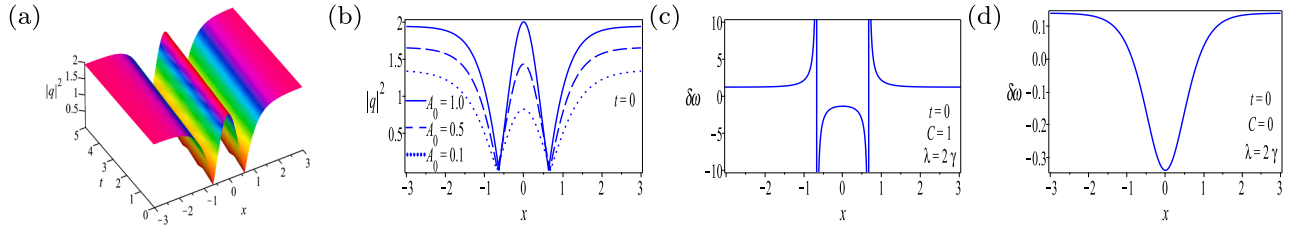

Fig. 1. (a)-(b) W-shaped soliton solution given by (22) and (c)-(d) profile of chirping presented in (23) with $a = 0.5, b = -0.5, \omega = 0.5, \nu = \sigma = 0.05, \gamma = 0.03, \lambda = -2\gamma/3, C = A_0 = 1$.

$$A_4 = \frac{C^2}{a^2}. \tag{12}$$

Due to the term of negative power in Eq. (8), we assume the variable transformation which is introduced as

$$u^2 = V, \tag{13}$$

so as to reduce Eq. (8) into the form

$$V'' + 4A_0 + 4A_1 V + 3A_2 V^2 + \frac{8}{3}A_3 V^3 = 0. \tag{14}$$

The structure of Eq. (14) is one of the prominent mathematical models which characterize many physical media. For example, Vyas et al. [39] and Saini et al. [40] studied higher order NLSE with self-steepening and self-frequency shift to investigate exact traveling wave solutions. The model is reduced to an elliptic equation of the form (14). In both studies, chirped chiral solitons are obtained and the effect of chirping is examined.

The elliptic Eq. (14) is known to possess abundant exact solutions which describe different types of physical phenomena. Herein, the combination of solutions to Eq. (14) along with the relations (2) and (13) leads to the general form of exact solutions for Eq. (1) presented as

$$q(x,t) = V^{1/2} e^{i(\phi(\xi) - \omega t)}, \tag{15}$$

where the function $\phi(\xi)$ representing the nonlinear phase shift can be found by integrating Eq. (17) with respect to ξ as

$$\phi(\xi) = \frac{(\nu + \sigma)}{2a}\xi - \int \left[\frac{(3\lambda + 2\gamma)}{4a} V + \frac{C}{aV}\right] \mathrm{d}\xi + \theta, \tag{16}$$

where θ is a constant phase. The chirp, which is expressed in terms of the nonlinear phase shift, has the form $\delta\omega(x,t) = -\frac{\partial}{\partial x}[\phi(\xi) - \Omega t] = -\phi'(\xi)$. Using (16), the chirping can be found as

$$\delta\omega(x,t) = -\frac{(\nu + \sigma)}{2a} + \frac{(3\lambda + 2\gamma)}{4a} V + \frac{C}{aV}. \tag{17}$$

3. W-shaped and various types of optical solitons

In what follows, we derive various types of exact solutions of the perturbed NLSE (1) be means of three different soliton ansatzes. This technique will be applied mainly to Eq. (14) and then the solution extracted will be substituted into (2) with the help of (13). The obtained solutions include W-shaped, bright, dark, kink, anti-kink and kink-dark solitons.

3.1. First soliton ansatz

We express that the solution of Eq. (14) has the form

$$V(\xi) = C_1 - C_2 \mathrm{sech}^2(m\xi), \tag{18}$$

where m and C_i, $(i = 1, 2)$ are constants to be determined. Inserting the ansatz (18) into Eq. (14), a polynomial in $\mathrm{sech}^n(m\xi)$, $(n = 0, 2, 4, 6)$ will be constructed. Equating each coefficient of $\mathrm{sech}^n(m\xi)$ in this polynomial to zero, yields a system of algebraic equations for m and C_i. Solving this system of equations, we can obtain the following values of m and C_i.

$$\begin{aligned} C_1 &= -\frac{2(A_1 + \sqrt{A_1^2 - 3A_0A_2})}{3A_2}, \\ C_2 &= -\frac{2\sqrt{A_1^2 - 3A_0A_2}}{A_2}, \\ m^4 &= A_1^2 - 3A_0A_2, \end{aligned} \tag{19}$$

with the constraint condition $A_3 = 0$ written in the model parameters as

$$\lambda = -\frac{2\gamma}{3}, \tag{20}$$

or

$$\lambda = 2\gamma. \tag{21}$$

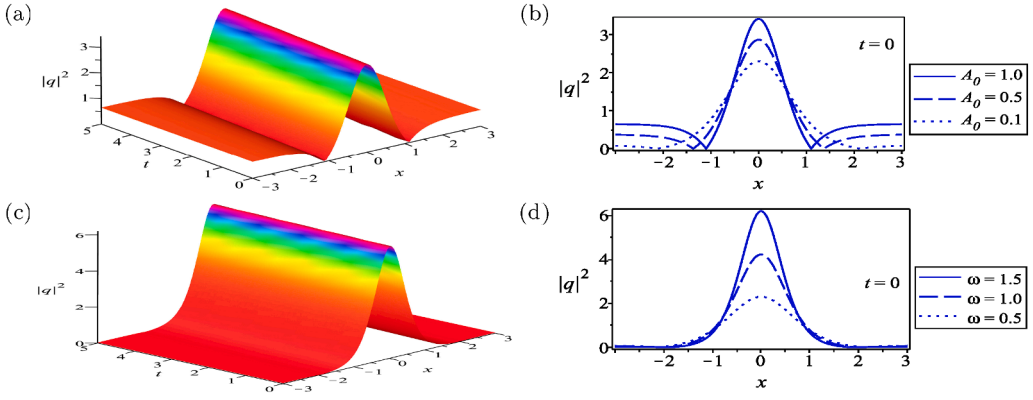

Fig. 2. W-shaped and bright soliton solution given by (22) with $a = -0.5, b = 0.5, \nu = \sigma = 0.05, \gamma = 0.03, \lambda = -2\gamma/3, C = 1$; for (a)-(b) $\omega = 0.5, A_0 = 1$ and for (c)-(d) $\omega. = 1.5, A_0 = 0.1$.

Substituting the values of parameters given in (19) into (18) along with using (13) and (2), we reach the optical soliton solution of (1) given by

$$q(x,t)=\left\{-\frac{2\sqrt{A_1^2-3A_0A_2}}{3A_2}\left[1+\frac{A_1}{\sqrt{A_1^2-3A_0A_2}}-3\mathrm{sech}^2\left(\left(A_1^2-3A_0A_2\right)^{1/4}\xi\right)\right]\right\}^{\frac{1}{2}}e^{i(\phi(\xi)-\omega t)}, \tag{22}$$

where $A_2<0$ and $A_1^2-3A_0A_2>0$ for the validity of optical solitons with real values for the pulse width and amplitude. The corresponding chirping is obtained as

$$\delta\omega(x,t)=-\frac{(\nu+\sigma)}{2a}-\frac{(3\lambda+2\gamma)}{6aA_2}\sqrt{A_1^2-3A_0A_2}\left[1+\frac{A_1}{\sqrt{A_1^2-3A_0A_2}}-3\mathrm{sech}^2\left(\left(A_1^2-3A_0A_2\right)^{1/4}\xi\right)\right]-\frac{3CA_2}{2a\sqrt{A_1^2-3A_0A_2}\left[1+\frac{A_1}{\sqrt{A_1^2-3A_0A_2}}-3\mathrm{sech}^2\left(\left(A_1^2-3A_0A_2\right)^{1/4}\xi\right)\right]}. \tag{23}$$

The solution (22) gives rise to W-shaped soliton which propagates in nano optical fibers. However, this wave is found to turn into either bright or dark optical solitons because of some limitations. For example, W-shaped solitons which are created under the condition $A_1<0$, $3A_0A_2<0$ degenerate to bright optical solitons as $A_1^2\gg|3A_0A_2|$. Similarly, although W-shaped soliton is constructed in the limit $A_1>0$, the condition $A_1>0, 3A_0A_2<A_1^2\le 4A_0A_2$ enables the formation of dark optical soliton only.

Figs. 1–3 show the dynamic behaviour of solution (22) which generates three types of soliton structures based on specific constraints stated above. For example, Fig. 1(a) exhibits the 3D plot for the propagation of W-shaped soliton where the plot is depicted by selecting appropriate values for the parameters given as $a=0.5, b=-0.5, \omega=0.5, \nu=\sigma=0.05, \gamma=0.03, \lambda=-2\gamma/3, C=A_0=1$. Note that the amplitude of waves changes according to the variation of parameter values as shown in Fig. 1(b). The behaviour of W-shaped soliton obeying the condition $A_1<0, 3A_0A_2<0$ is described in Fig. 2(a)-(b) with the values $a=-0.5, b=\omega=0.5, \nu=\sigma=0.05, \gamma=0.03, \lambda=-2\gamma/3, C=A_0=1$. Following the same condition and once $A_1^2\gg|3A_0A_2|$, the bright soliton is demonstrated in Fig. 2(c)-(d) with the same value of parameters but $\omega=1.5, A_0=0.1$. Fig. 3 illustrates the evolution of dark soliton with $a=0.5, b=-0.5, \omega=1, \nu=\sigma=0.05, \gamma=0.08, \lambda=2\gamma, C=-1.5, A_0=-2.5$. It is clear that the dark soliton evanesces near the lower boundary of $3A_0A_2<A_1^2\le 4A_0A_2$ as presented by the solid line of Fig. 3(b). The profile of chirping is shown in Fig. 1(c)-(d).

It is worth mentioning that the case $A_0=0$ (i.e., neglecting the constant of integration in Eq. (14)) reduces the optical soliton solution (22) to the form

$$q(x,t)=\left\{-\frac{4A_1}{3A_2}\left[1-\frac{3}{2}\mathrm{sech}^2\left(\sqrt{A_1}\,\xi\right)\right]\right\}^{\frac{1}{2}}e^{i(\phi(\xi)-\omega t)}, \tag{24}$$

which demands $A_1>0$ and $A_2<0$. The chirping is derived as

$$\delta\omega(x,t)=-\frac{(\nu+\sigma)}{2a}-\frac{(3\lambda+2\gamma)A_1}{3aA_2}\left[1-\frac{3}{2}\mathrm{sech}^2\left(\sqrt{A_1}\,\xi\right)\right]-\frac{3CA_2}{4aA_1\left[1-\frac{3}{2}\mathrm{sech}^2\left(\sqrt{A_1}\,\xi\right)\right]}. \tag{25}$$

The soliton solution (24) represents a form of W-shaped soliton which is in agreement with the structure of W-shaped soliton solution

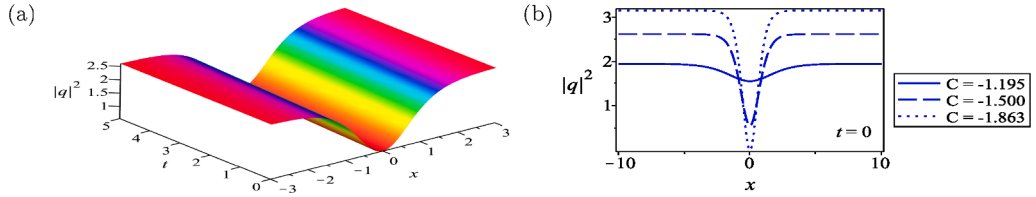

Fig. 3. Dark soliton solution given by (22) with $a=0.5, b=-0.5, \omega=1, \nu=\sigma=0.05, \gamma=0.08, \lambda=2\gamma, C=-1.5, A_0=-2.5$.

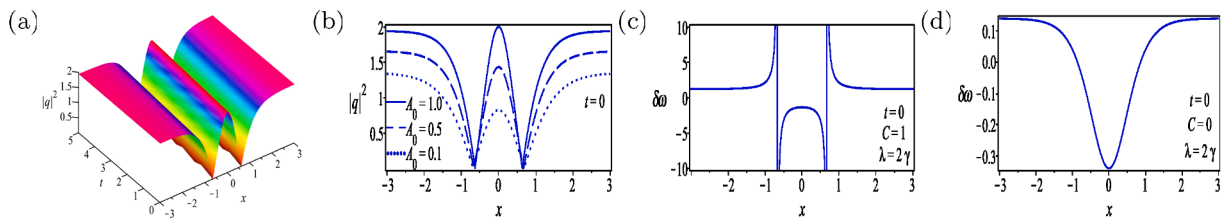

Fig. 4. (a)-(b) W-shaped soliton solution given by (30) and (c)-(d) profile of chirping presented in (31) with $a = \omega = 0.5, b = -0.5, \nu = \sigma = 0.05, \gamma = 0.03, \lambda = -2\gamma/3, C = A_0 = 1$.

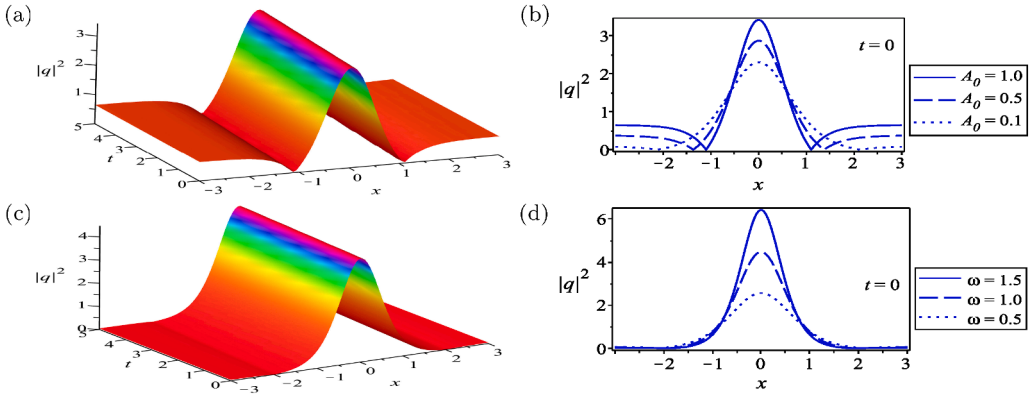

Fig. 5. W-shaped and bright soliton solution given by (30) with $a = -0.5, b = 0.5, \nu = \sigma = 0.05, \gamma = 0.03, \lambda = -2\gamma/3, C = 1$; for (a)-(b) $\omega = 0.5, A_0 = 1$ and for (c)-(d) $\omega = 1, A_0 = 0.1$.

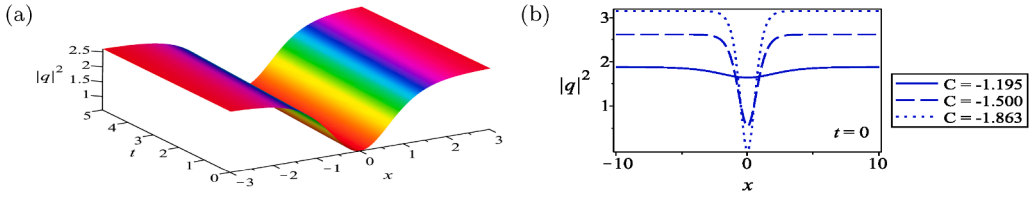

Fig. 6. Dark soliton solution given by (30) with $a = 0.5, b = -0.5, \omega = 1, \nu = \sigma = 0.05, \gamma = 0.08, \lambda = 2\gamma, C = -1.5, A_0 = -2.5$.

derived by authors in reference [38].

On the other hand, if $A_1 < 0$ and $A_2 > 0$, we arrive at an exact solution to Eq. (1) describing the bright optical soliton given by

$$q(x,t) = \sqrt{-\frac{2A_1}{A_2}}\,\mathrm{sech}\left(\sqrt{-A_1}\,\xi\right)e^{i(\phi(\xi)-\omega t)}, \tag{26}$$

where the associated chirp reads

$$\delta\omega(x,t) = -\frac{(\nu+\sigma)}{2a} + \frac{(3\lambda+2\gamma)}{4a}\sqrt{-\frac{2A_1}{A_2}}\,\mathrm{sech}\left(\sqrt{-A_1}\,\xi\right) + \frac{C}{a\sqrt{-\frac{2A_1}{A_2}}\,\mathrm{sech}\left(\sqrt{-A_1}\,\xi\right)}. \tag{27}$$

3.2. Second soliton ansatz

Here, we consider that the elliptic Eq. (14) has an exact soliton solution in the form

$$V(\xi) = F_1 - \frac{F_2\,\mathrm{sech}(r\xi)}{1+\mathrm{sech}(r\xi)}, \tag{28}$$

where r and F_j, $(j = 1, 2)$ are constants to be determined. Plugging the ansatz (28) into Eq. (14), we arrive at a set of algebraic equations by equating the coefficients of various powers of $\mathrm{sech}(r\xi)$ to zero. Solving these algebraic equations, we obtain

$$F_1 = -\frac{2(A_1 + \sqrt{A_1^2 - 3A_0A_2})}{3A_2}, \quad F_2 = -\frac{4\sqrt{A_1^2 - 3A_0A_2}}{A_2}, \quad r^4 = 16(A_1^2 - 3A_0A_2), \tag{29}$$

with the same constraint conditions given in (20) or (21). The use of (2), (13) and (28) together with (29) leads to the formation of optical soliton solution to Eq. (1) given as

$$q(x,t) = \left\{ -\frac{2\sqrt{A_1^2 - 3A_0A_2}}{3A_2}\left[1 + \frac{A_1}{\sqrt{A_1^2 - 3A_0A_2}} - \frac{6\,\mathrm{sech}\left(2\left(A_1^2 - 3A_0A_2\right)^{1/4}\xi\right)}{1+\mathrm{sech}\left(2\left(A_1^2 - 3A_0A_2\right)^{1/4}\xi\right)}\right]\right\}^{\frac{1}{2}} e^{i(\phi(\xi)-\omega t)}, \tag{30}$$

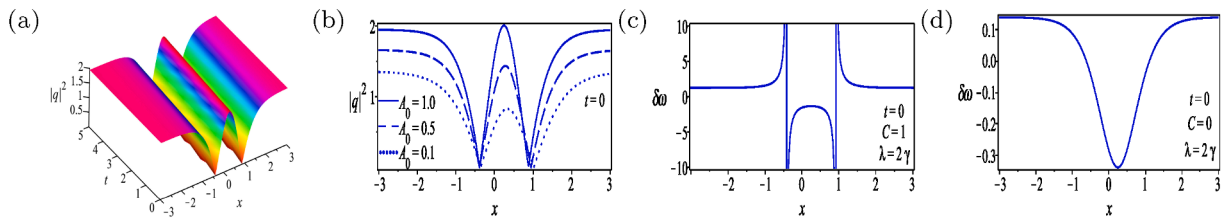

Fig. 7. (a)-(b) W-shaped soliton solution given by (38) and (c)-(d) profile of chirping presented in (39) with $a = \omega = 0.5, b = -0.5, \nu = \sigma = 0.05, \gamma = 0.03, \lambda = -2\gamma/3, C = 1, A_0 = 1$.

which is valid when $A_2 < 0$ and $A_1^2 - 3A_0A_2 > 0$. The associated chirp is extracted as

$$\delta\omega(x,t) = -\frac{(\nu+\sigma)}{2a} - \frac{(3\lambda+2\gamma)}{6aA_2}\sqrt{A_1^2-3A_0A_2}\left[1+\frac{A_1}{\sqrt{A_1^2-3A_0A_2}} - \frac{6\mathrm{sech}\left(2\left(A_1^2-3A_0A_2\right)^{1/4}\xi\right)}{1+\mathrm{sech}\left(2\left(A_1^2-3A_0A_2\right)^{1/4}\xi\right)}\right] - \frac{3CA_2}{2a\sqrt{A_1^2-3A_0A_2}\left[1+\frac{A_1}{\sqrt{A_1^2-3A_0A_2}} - \frac{6\mathrm{sech}\left(2\left(A_1^2-3A_0A_2\right)^{1/4}\xi\right)}{1+\mathrm{sech}\left(2\left(A_1^2-3A_0A_2\right)^{1/4}\xi\right)}\right]}. \tag{31}$$

This solution represents the propagation of W-shaped soliton which is subject to change into bright or dark solitons due to the same conditions stated before. Inevitably, the bright and dark solitons are formed under the conditions $A_1 < 0, A_1^2 \gg |3A_0A_2|$ and $A_1 > 0$, $3A_0A_2 < A_1^2 \leq 4A_0A_2$, respectively.

Figs. 4–6 present the evolution of solution (30) which yields three shapes of solitons demonstrated as follows. Fig. 4 shows the behaviour of W-shaped soliton for the same values of parameters as in Fig. 1, where the 2D plot in Fig. 4(b) describes the variations of W-shaped pulses by altering the value of A_0. Under the condition $A_1 < 0, 3A_0A_2 < 0$ and using the same values of parameters as in Fig. 2, the propagation of W-shaped soliton is illustrated in Fig. 5(a)-(b). This structure degenerates to the bright soliton when $A_1^2 \gg |3A_0A_2|$ as shown in Fig. 5(c)-(d). Fig. 6 depicts the dark soliton which solely exists at the condition $A_1 > 0$, $3A_0A_2 < A_1^2 \leq 4A_0A_2$. The corresponding chirping is illustrated in Fig. 4 (c)-(d).

In case of $A_0 = 0$, the optical soliton solution (30) is converted purely to W-shaped soliton written as

$$q(x,t) = \left\{-\frac{4A_1}{3A_2}\left[1-\frac{3\mathrm{sech}\left(2\sqrt{A_1}\,\xi\right)}{1+\mathrm{sech}\left(2\sqrt{A_1}\,\xi\right)}\right]\right\}^{\frac{1}{2}} e^{i(\phi(\xi)-\omega t)}, \tag{32}$$

which needs $A_1 > 0$ and $A_2 < 0$. The chirp expression is addressed as

$$\delta\omega(x,t) = -\frac{(\nu+\sigma)}{2a} - \frac{(3\lambda+2\gamma)A_1}{3aA_2}\left[1-\frac{3\mathrm{sech}\left(2\sqrt{A_1}\,\xi\right)}{1+\mathrm{sech}\left(2\sqrt{A_1}\,\xi\right)}\right] - \frac{3CA_2}{4aA_1\left[1-\frac{3\mathrm{sech}\left(2\sqrt{A_1}\,\xi\right)}{1+\mathrm{sech}\left(2\sqrt{A_1}\,\xi\right)}\right]}. \tag{33}$$

This form of W-shaped soliton corresponds to the one obtained by Triki et al. [38]. On the contrary, when $A_1 < 0$ and $A_2 > 0$, we reach an exact bright optical soliton solution to Eq. (1) given by

$$q(x,t) = \left\{-\frac{4A_1}{3A_2}\frac{\mathrm{sech}\left(2\sqrt{-A_1}\,\xi\right)}{1+\mathrm{sech}\left(2\sqrt{-A_1}\,\xi\right)}\right\}^{\frac{1}{2}} e^{i(\phi(\xi)-\omega t)}, \tag{34}$$

while the corresponding chirping is obtained as

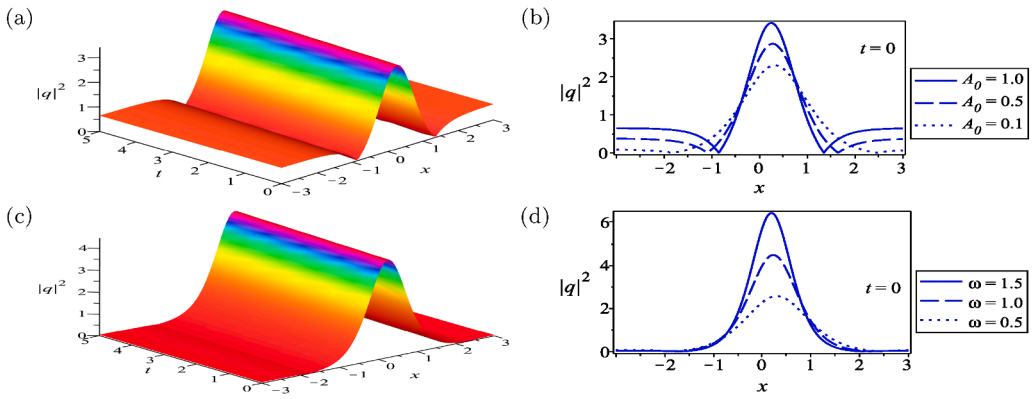

Fig. 8. W-shaped and bright soliton solution given by (38) with $a = -0.5, b = 0.5, \nu = \sigma = 0.05, \gamma = 0.03, \lambda = -2\gamma/3, C = 1$; for (a)-(b) $\omega = 0.5, A_0 = 1$ and for (c)-(d) $\omega = 1, A_0 = 0.1$.

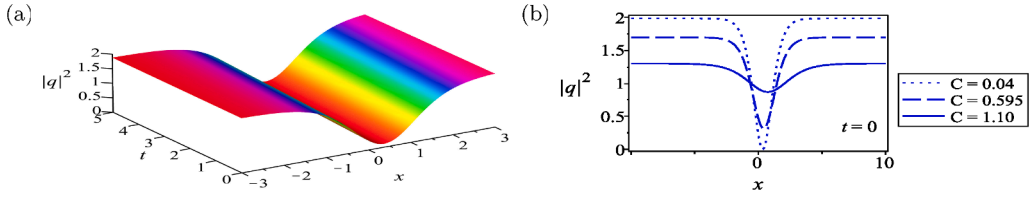

Fig. 9. Dark soliton solution given by (38) with $a = 0.5, b = -0.5, \omega = C = 1, \nu = \sigma = 0.05, \gamma = 0.03, \lambda = 2\gamma, A_0 = -1$.

$$\delta\omega(x,t) = -\frac{(\nu+\sigma)}{2a} - \frac{(3\lambda+2\gamma)A_1}{3aA_2}\left[\frac{\operatorname{sech}\left(2\sqrt{A_1}\,\xi\right)}{1+\operatorname{sech}\left(2\sqrt{A_1}\,\xi\right)}\right] - \frac{3CA_2}{4aA_1}\left[\frac{1+\operatorname{sech}\left(2\sqrt{A_1}\,\xi\right)}{\operatorname{sech}\left(2\sqrt{A_1}\,\xi\right)}\right]. \tag{35}$$

3.3. Third soliton ansatz

We assume that Eq. (14) has an exact optical soliton solution in the form

$$V(\xi) = H_1 - \frac{H_2\operatorname{sech}^2(s\xi)}{4-[1-\tanh(s\xi)]^2} + \frac{H_3\operatorname{sech}^4(s\xi)}{(4-[1-\tanh(s\xi)]^2)^2}, \tag{36}$$

where s and H_l, $(l = 1,2,3)$ are constants to be determined. Substituting the ansatz (36) into Eq. (14) and equating all coefficients having the same order of $\operatorname{sech}(s\xi)\tanh(s\xi)$ to zero, gives us a set of algebraic equations that induces different cases of solutions for the parameters s and H_l.

Case I.

$$\begin{aligned} H_1 &= -\frac{2(A_1+\sqrt{A_1^2-3A_0A_2})}{3A_2}, \\ H_2 &= -\frac{16\sqrt{A_1^2-3A_0A_2}}{A_2}, \\ H_3 &= -\frac{32\sqrt{A_1^2-3A_0A_2}}{A_2}, \\ s^4 &= A_1^2-3A_0A_2. \end{aligned} \tag{37}$$

These values are extracted under the same constraints given in (20) or (21). Employing (2) and (36) together with (37), we come up with optical soliton solution to Eq. (1) written as

$$q(x,t) = \left\{ -\frac{2\sqrt{A_1^2-3A_0A_2}}{3A_2}\left[1+\frac{A_1}{\sqrt{A_1^2-3A_0A_2}} - \frac{24\operatorname{sech}^2\left((A_1^2-3A_0A_2)^{1/4}\xi\right)}{4-\left[1-\tanh\left((A_1^2-3A_0A_2)^{1/4}\xi\right)\right]^2} + \frac{48\operatorname{sech}^4\left((A_1^2-3A_0A_2)^{1/4}\xi\right)}{\left(4-\left[1-\tanh\left((A_1^2-3A_0A_2)^{1/4}\xi\right)\right]^2\right)^2}\right]\right\}^{\frac{1}{2}} e^{i(\phi(\xi)-\omega t)}, \tag{38}$$

provided that $A_2 < 0$ and $A_1^2 - 3A_0A_2 > 0$. The corresponding chirping takes the form

$$\delta\omega(x,t) = -\frac{(\nu+\sigma)}{2a} - \frac{(3\lambda+2\gamma)}{6aA_2}\sqrt{A_1^2-3A_0A_2}\left[1+\frac{A_1}{\sqrt{A_1^2-3A_0A_2}} - \frac{24\,\mathrm{sech}^2\left((A_1^2-3A_0A_2)^{1/4}\xi\right)}{4-\left[1-\tanh\left((A_1^2-3A_0A_2)^{1/4}\xi\right)\right]^2} + \frac{48\,\mathrm{sech}^4\left((A_1^2-3A_0A_2)^{1/4}\xi\right)}{\left(4-\left[1-\tanh\left((A_1^2-3A_0A_2)^{1/4}\xi\right)\right]^2\right)^2}\right] - \frac{3CA_2}{2a\sqrt{A_1^2-3A_0A_2}} \times \frac{1}{\left[1+\frac{A_1}{\sqrt{A_1^2-3A_0A_2}} - \frac{24\,\mathrm{sech}^2\left((A_1^2-3A_0A_2)^{1/4}\xi\right)}{4-\left[1-\tanh\left((A_1^2-3A_0A_2)^{1/4}\xi\right)\right]^2} + \frac{48\,\mathrm{sech}^4\left((A_1^2-3A_0A_2)^{1/4}\xi\right)}{\left(4-\left[1-\tanh\left((A_1^2-3A_0A_2)^{1/4}\xi\right)\right]^2\right)^2}\right]}. \tag{39}$$

The behaviour of solution (38) is exhibited in Figs. 7–9 which show the plots of three types of waves including W-shaped, bright and dark solitons. Fig. 7 displays the evolution of W-shaped soliton with the same values of parameters as in Fig. 1. The structure of W-shaped wave dominated by the constraint $A_1 < 0, 3A_0A_2 < 0$ is demonstrated in Fig. 8 (a)-(b) with the same values of parameters as in Fig. 2. As the parameters reaching the limit $A_1 < 0, A_1^2 \gg |3A_0A_2|$, the bright soliton pulse emerges in nano optical fibers and it is plotted in Fig. 8(c)-(d). The dark soliton which arises due to the restriction of $A_1 > 0, 3A_0A_2 < A_1^2 \leq 4A_0A_2$ is illustrated in Fig. 9. The chirping profile is shown in Fig. 7(c)-(d).

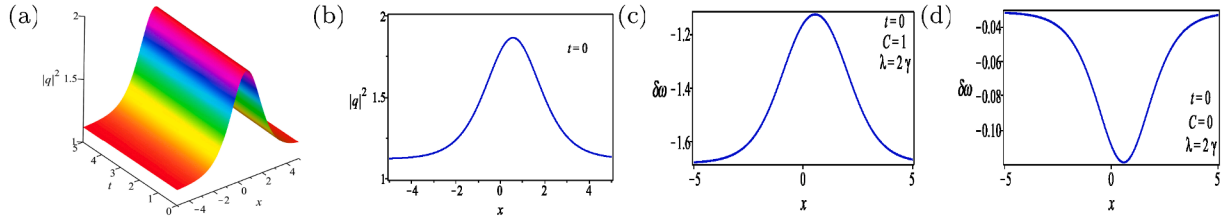

Fig. 10. (a)-(b) Bright soliton solution given by (45) and (c)-(d) profile of chirping presented in (46) with $a = b = -0.5, \omega = C = 1, \nu = \sigma = 0.05, \gamma = 0.03, \lambda = -2\gamma/3$.

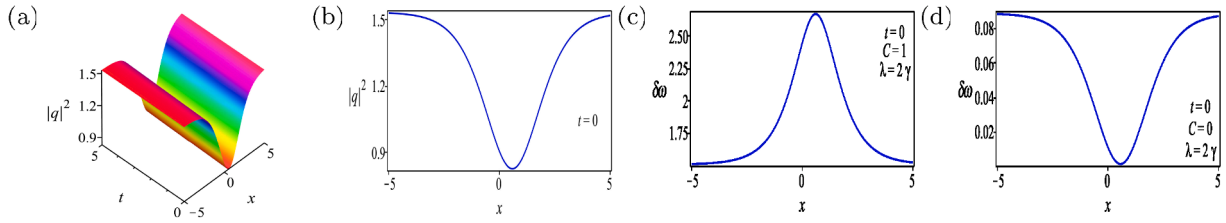

Fig. 11. (a)-(b) Dark soliton solution given by (48) and (c)-(d) profile of chirping presented in (49) with $a = 0.5, b = -0.5, \omega = C = 1, \nu = \sigma = 0.05, \gamma = 0.03, \lambda = -2\gamma/3$.

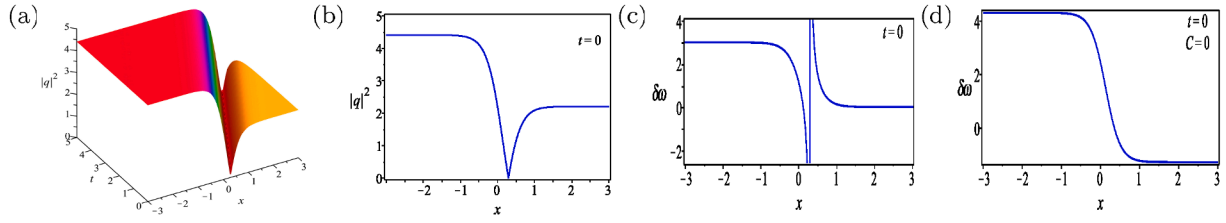

Fig. 12. (a)-(b) Kink-dark soliton solution given by (53) and (c)-(d) profile of chirping presented in (54) with $a = -0.5, b = \omega = \nu = \gamma = 0.5, \sigma = \lambda = 0.1$.

Analogous to the solutions (22) and (30) it is found that the soliton solution (38) characterizes the propagation of W-shaped soliton. In addition to this, the W-shaped soliton wave undergoes a collapse to form bright and dark solitons under the same restrictions mentioned before, where the former is created when $A_1 < 0, A_1^2 \gg |3A_0A_2|$ whereas the latter is formed at $A_1 > 0, 3A_0A_2 < A_1^2 \leq 4A_0A_2$.

Case II. Based on the assumption $A_0 = 0$, the optical soliton solution (38) becomes in the form

$$q(x,t) = \left\{ -\frac{4A_1}{3A_2}\left[1 - \frac{12\mathrm{sech}^2\left(\sqrt{A_1}\,\xi\right)}{4 - \left[1 - \tanh\left(\sqrt{A_1}\,\xi\right)\right]^2} + \frac{24\mathrm{sech}^4\left(\sqrt{A_1}\,\xi\right)}{\left(4 - \left[1 - \tanh\left(\sqrt{A_1}\,\xi\right)\right]^2\right)^2}\right]\right\}^{\frac{1}{2}} e^{i(\phi(\xi)-\omega t)}, \tag{40}$$

where $A_1 > 0$ and $A_2 < 0$. The chirp form is obtained as

$$\delta\omega(x,t) = -\frac{(\nu+\sigma)}{2a} - \frac{(3\lambda+2\gamma)A_1}{3aA_2}\left[1 - \frac{12\mathrm{sech}^2\left(\sqrt{A_1}\,\xi\right)}{4 - \left[1 - \tanh\left(\sqrt{A_1}\,\xi\right)\right]^2} + \frac{24\mathrm{sech}^4\left(\sqrt{A_1}\,\xi\right)}{\left(4 - \left[1 - \tanh\left(\sqrt{A_1}\,\xi\right)\right]^2\right)^2}\right] - \frac{3CA_2}{4aA_1\left[1 - \frac{12\mathrm{sech}^2\left(\sqrt{A_1}\,\xi\right)}{4 - \left[1 - \tanh\left(\sqrt{A_1}\,\xi\right)\right]^2} + \frac{24\mathrm{sech}^4\left(\sqrt{A_1}\,\xi\right)}{\left(4 - \left[1 - \tanh\left(\sqrt{A_1}\,\xi\right)\right]^2\right)^2}\right]}. \tag{41}$$

This optical soliton embodies merely a structure of W-shaped soliton which matches its counterpart in [38]. As $A_1 < 0$ and $A_2 > 0$, the term with parameter H_1 will vanish from (36) and this leads to an exact bright optical soliton given by

$$q(x,t) = \left\{ -\frac{16A_1}{A_2}\left[\frac{\mathrm{sech}^2\left(\sqrt{-A_1}\,\xi\right)}{4 - \left[1 - \tanh\left(\sqrt{-A_1}\,\xi\right)\right]^2} - \frac{2\mathrm{sech}^4\left(\sqrt{-A_1}\,\xi\right)}{\left(4 - \left[1 - \tanh\left(\sqrt{-A_1}\,\xi\right)\right]^2\right)^2}\right]\right\}^{\frac{1}{2}} e^{i(\phi(\xi)-\omega t)}, \tag{42}$$

whereas the associated chirp is presented as

$$\delta\omega(x,t) = -\frac{(\nu+\sigma)}{2a} - \frac{4(3\lambda+2\gamma)A_1}{aA_2}\left[\frac{\mathrm{sech}^2\left(\sqrt{-A_1}\,\xi\right)}{4 - \left[1 - \tanh\left(\sqrt{-A_1}\,\xi\right)\right]^2} - \frac{2\mathrm{sech}^4\left(\sqrt{-A_1}\,\xi\right)}{\left(4 - \left[1 - \tanh\left(\sqrt{-A_1}\,\xi\right)\right]^2\right)^2}\right] - \frac{CA_2}{16aA_1\left[\frac{\mathrm{sech}^2\left(\sqrt{-A_1}\,\xi\right)}{4 - \left[1 - \tanh\left(\sqrt{-A_1}\,\xi\right)\right]^2} - \frac{2\mathrm{sech}^4\left(\sqrt{-A_1}\,\xi\right)}{\left(4 - \left[1 - \tanh\left(\sqrt{-A_1}\,\xi\right)\right]^2\right)^2}\right]}. \tag{43}$$

In this case, the constraints given by (20) or (21) must stay valid in order for the W-shaped and bright optical solitons to exist.

Case III. Under the restrictions given by (20) or (21) and $121A_0A_2 = 39A_1^2$, we come by the following two sets of constant values.

Set 1.

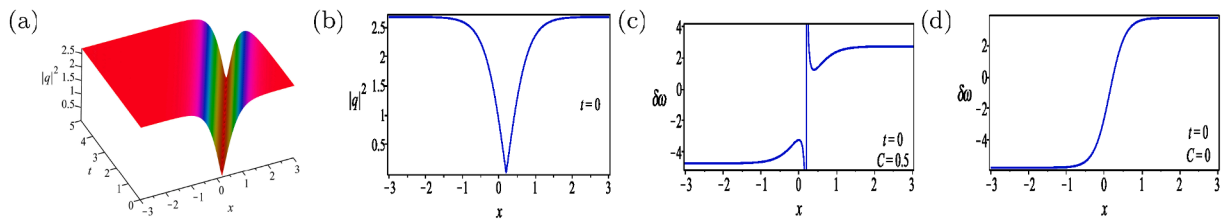

Fig. 13. (a)-(b) Dark soliton solution given by (57) and (c)-(d) profile of chirping presented in (58) with $a = b = \omega = \nu = \gamma. = \sigma = C = 0.5$.

$$\begin{aligned} H_1 &= -\frac{6A_1}{11A_2}, \\ H_2 &= \frac{32A_1}{11A_2}, \\ H_3 &= \frac{64A_1}{11A_2}, \\ s &= \sqrt{-\frac{2A_1}{11}}, \end{aligned} \tag{44}$$

As a consequence of utilizing these findings, one can obtain an exact bright optical soliton solution to Eq. (1) written as

$$q(x,t) = \left\{ -\frac{2A_1}{11A_2}\left[3 + \frac{16\mathrm{sech}^2\left(\sqrt{-\frac{2A_1}{11}}\xi\right)}{4 - \left[1 - \tanh\left(\sqrt{-\frac{2A_1}{11}}\xi\right)\right]^2} - \frac{32\mathrm{sech}^4\left(\sqrt{-\frac{2A_1}{11}}\xi\right)}{\left(4 - \left[1 - \tanh\left(\sqrt{-\frac{2A_1}{11}}\xi\right)\right]^2\right)^2} \right] \right\}^{\frac{1}{2}} e^{i(\phi(\xi)-\omega t)}, \tag{45}$$

provided that $A_1 < 0$ and $A_2 > 0$. Consequently, the chirping is given by

$$\begin{aligned} \delta\omega(x,t) = &-\frac{(\nu+\sigma)}{2a} - \frac{(3\lambda+2\gamma)A_1}{22aA_2}\left[3 + \frac{16\mathrm{sech}^2\left(\sqrt{-\frac{2A_1}{11}}\xi\right)}{4 - \left[1 - \tanh\left(\sqrt{-\frac{2A_1}{11}}\xi\right)\right]^2} - \frac{32\mathrm{sech}^4\left(\sqrt{-\frac{2A_1}{11}}\xi\right)}{\left(4 - \left[1 - \tanh\left(\sqrt{-\frac{2A_1}{11}}\xi\right)\right]^2\right)^2} \right] \\ &\frac{11CA_2}{2aA_1\left[3 + \frac{16\mathrm{sech}^2\left(\sqrt{-\frac{2A_1}{11}}\xi\right)}{4 - \left[1 - \tanh\left(\sqrt{-\frac{2A_1}{11}}\xi\right)\right]^2} - \frac{32\mathrm{sech}^4\left(\sqrt{-\frac{2A_1}{11}}\xi\right)}{\left(4 - \left[1 - \tanh\left(\sqrt{-\frac{2A_1}{11}}\xi\right)\right]^2\right)^2} \right]}. \end{aligned} \tag{46}$$

Fig. 10 shows the behaviour of solution (45) with different values of parameters given as $a = b = -0.5, \omega = C = 1, \nu = \sigma = 0.05, \gamma = 0.03$, $\lambda = -2\gamma/3$. It can be seen that this solution describes the bright soliton wave. The graph of associated chirp is displayed in Fig. 10(c)-(d).

Set 2.

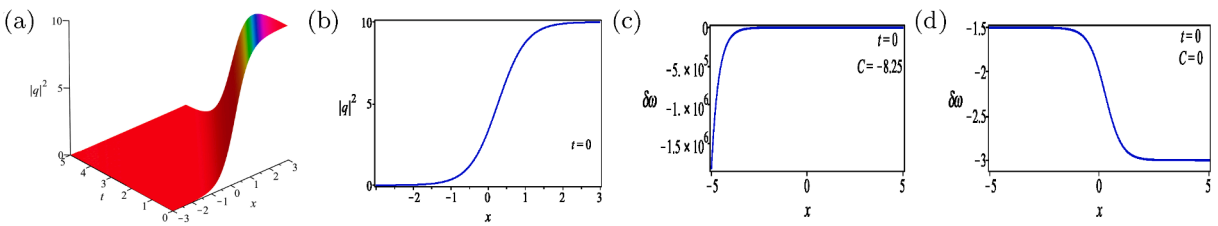

Fig. 14. (a)-(b) Kink soliton solution given by (61) and (c)-(d) profile of chirping presented in (62) with $a = b = \sigma = 0.5, \omega = \nu = 1, \gamma = -0.3, \lambda = 0.1$.

$$H_1 = -\frac{26A_1}{33A_2},$$
$$H_2 = -\frac{32A_1}{11A_2},$$
$$H_3 = -\frac{64A_1}{11A_2},$$
$$s = \sqrt{\frac{2A_1}{11}}, \tag{47}$$

which can be inserted into (36) to provide the soliton solution of Eq. (1) as

$$q(x,t) = \left\{ -\frac{2A_1}{33A_2}\left[13 - \frac{48\mathrm{sech}^2\left(\sqrt{\frac{2A_1}{11}}\xi\right)}{4-\left[1-\tanh\left(\sqrt{\frac{2A_1}{11}}\xi\right)\right]^2} + \frac{96\mathrm{sech}^4\left(\sqrt{\frac{2A_1}{11}}\xi\right)}{\left(4-\left[1-\tanh\left(\sqrt{\frac{2A_1}{11}}\xi\right)\right]^2\right)^2}\right]\right\}^{\frac{1}{2}} e^{i(\phi(\xi)-\omega t)}, \tag{48}$$

provided that $A_1 > 0$ and $A_2 < 0$. The corresponding chirp takes the form

$$\delta\omega(x,t) = -\frac{(\nu+\sigma)}{2a} - \frac{(3\lambda+2\gamma)A_1}{66aA_2}\left[13 - \frac{48\mathrm{sech}^2\left(\sqrt{\frac{2A_1}{11}}\xi\right)}{4-\left[1-\tanh\left(\sqrt{\frac{2A_1}{11}}\xi\right)\right]^2} + \frac{96\mathrm{sech}^4\left(\sqrt{\frac{2A_1}{11}}\xi\right)}{\left(4-\left[1-\tanh\left(\sqrt{\frac{2A_1}{11}}\xi\right)\right]^2\right)^2}\right]$$
$$-\frac{33CA_2}{2aA_1\left[13 - \frac{48\mathrm{sech}^2\left(\sqrt{\frac{2A_1}{11}}\xi\right)}{4-\left[1-\tanh\left(\sqrt{\frac{2A_1}{11}}\xi\right)\right]^2} + \frac{96\mathrm{sech}^4\left(\sqrt{\frac{2A_1}{11}}\xi\right)}{\left(4-\left[1-\tanh\left(\sqrt{\frac{2A_1}{11}}\xi\right)\right]^2\right)^2}\right]}. \tag{49}$$

Fig. 11 shows the behaviour of solution (48) which represents dark soliton wave. The plots are depicted by selecting the values of parameters as $a = 0.5, b = -0.5, \omega = C = 1, \nu = \sigma = 0.05, \gamma = 0.03, \lambda = -2\gamma/3$. The profile of corresponding chirping is exhibited in Fig. 11(c)-(d).

Case IV. Neglecting the last term in (36), i.e. $H_3 = 0$, we end up with the parameter values

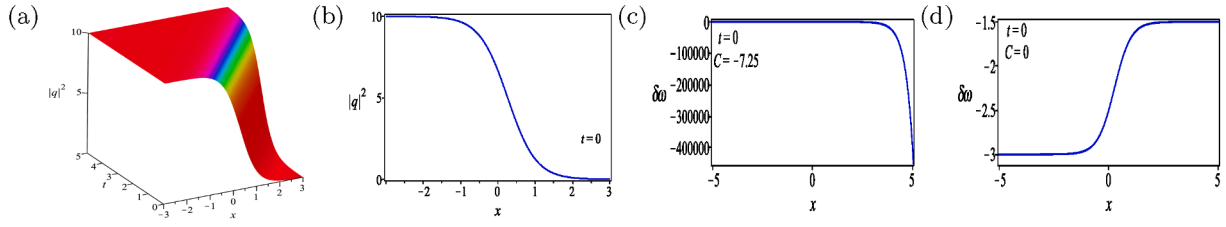

Fig. 15. (a)-(b) Anti-kink soliton solution given by (63) and (c)-(d) profile of chirping presented in (64) with $a = b = \omega = \sigma = 0.5, \nu = 1, \gamma = -0.3, \lambda = 0.1$.

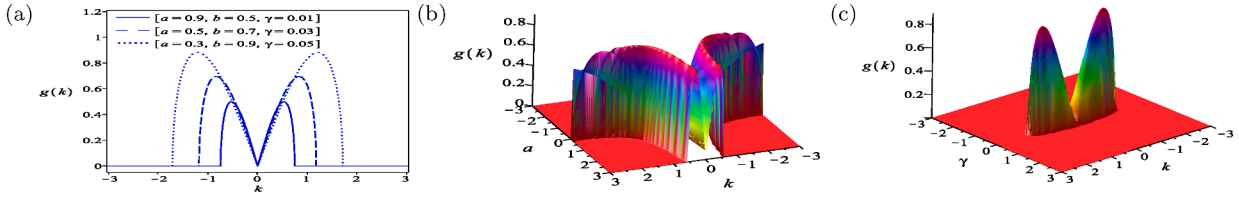

Fig. 16. Gain spectrum of modulation instability for different values of the parameters together with the relation $\lambda = 2\gamma$ and fixed value of incidence power taken as $P = 0.5$.

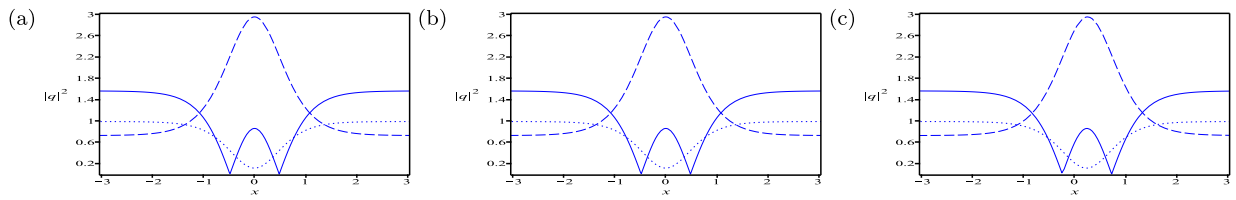

Fig. 17. The transition of wave profile from W-shaped soliton to bright and dark solitons for solutions given by (22), (30), (38) with $a = \gamma = C = 0.3, \sigma = 0.5$. (solid) $b = \nu = 0.5, \omega = -0.5, A_0 = 0.1$; (dash) $b = 0.5, \nu = \omega = -0.5, A_0 = 2$; (dot) $b = -0.5, \nu = \omega = 0.5, A_0 = -1.5$.

$$\begin{aligned} H_1 &= -\frac{4A_1}{3A_2}, \\ H_2 &= -\frac{8A_1}{A_2}, \\ s &= \sqrt{3A_1}, \end{aligned} \tag{50}$$

which is subject to the constraints $9A_0A_2 = -8A_1^2$ and $16A_1A_3 = -9A_2^2$. These constraints can be expressed in terms of the physical parameters as

$$A_0 = -\frac{4[2a\omega + (\nu+\sigma)^2 - C(\lambda+2\gamma)]^2}{9a^2[2ab - \lambda(\nu+\sigma)]}, \tag{51}$$

$$C = \frac{9[2ab - \lambda(\nu+\sigma)]^2 - 2(\lambda-2\gamma)(3\lambda+2\gamma)[2a\omega + (\nu+\sigma)^2]}{2(\lambda^2 - 4\gamma^2)(3\lambda+2\gamma)}. \tag{52}$$

Employing the obtained outcomes give rise to a new exact soliton solution to Eq. (1) describing kink-dark optical soliton in the form

$$q(x,t) = \left\{ -\frac{4A_1}{3A_2}\left[1 - \frac{6\mathrm{sech}^2\left(\sqrt{3A_1}\,\xi\right)}{4 - \left[1 - \tanh\left(\sqrt{3A_1}\,\xi\right)\right]^2}\right]\right\}^{\frac{1}{2}} e^{i(\phi(\xi) - \omega t)}, \tag{53}$$

which is valid for $A_1 > 0$ and $A_2 < 0$. The associated chirp is obtained as

$$\delta\omega(x,t) = -\frac{(\nu+\sigma)}{2a} - \frac{(3\lambda+2\gamma)A_1}{3aA_2}\left[1 - \frac{6\mathrm{sech}^2\left(\sqrt{3A_1}\,\xi\right)}{4 - \left[1 - \tanh\left(\sqrt{3A_1}\,\xi\right)\right]^2}\right] - \frac{3CA_2}{4aA_1\left[1 - \frac{6\mathrm{sech}^2\left(\sqrt{3A_1}\,\xi\right)}{4 - \left[1 - \tanh\left(\sqrt{3A_1}\,\xi\right)\right]^2}\right]}. \tag{54}$$

The soliton solution (53) is presented in Fig. 12 by choosing the values of parameters as $a = -0.5, b = \omega = \nu = \gamma = 0.5, \sigma = \lambda = 0.1$. The figure represents the structure of kink-dark soliton. The chirping profile is given in Fig. 12(c)-(d).

Case V. In addition to Case II obtained after considering $A_0 = 0$, we also arrive at

$$\begin{aligned} H_1 &= \frac{1}{2}\sqrt{-\frac{6A_1}{A_3}}, \\ H_2 &= 2\sqrt{-\frac{6A_1}{A_3}}, \\ H_3 &= 0, \\ s &= \sqrt{2A_1}, \end{aligned} \tag{55}$$

with the constraint $A_2 = 0$ which can be reverted to model parameters as

$$\lambda = \frac{2ab}{\nu+\sigma}. \tag{56}$$

Making use of all obtained constant values and parametric constraints, we acquire a new exact solution to Eq. (1) in the form

$$q(x,t) = \left\{\sqrt{-\frac{3A_1}{2A_3}}\left[1 - \frac{4\mathrm{sech}^2\left(\sqrt{2A_1}\,\xi\right)}{4 - \left[1 - \tanh\left(\sqrt{2A_1}\,\xi\right)\right]^2}\right]\right\}^{\frac{1}{2}} e^{i(\phi(\xi) - \omega t)}, \tag{57}$$

which implies $A_1 > 0$ and $A_3 < 0$. The corresponding chirping is given by

$$\delta\omega(x,t) = -\frac{(\nu+\sigma)}{2a} + \frac{(3\lambda+2\gamma)}{4a}\sqrt{-\frac{3A_1}{2A_3}}\left[1 - \frac{4\mathrm{sech}^2\left(\sqrt{2A_1}\,\xi\right)}{4 - \left[1 - \tanh\left(\sqrt{2A_1}\,\xi\right)\right]^2}\right] + \frac{C}{a\sqrt{-\frac{3A_1}{2A_3}}\left[1 - \frac{4\mathrm{sech}^2\left(\sqrt{2A_1}\,\xi\right)}{4 - \left[1 - \tanh\left(\sqrt{2A_1}\,\xi\right)\right]^2}\right]}. \tag{58}$$

The evolution of this solution is depicted in Fig. 13 with the values of parameters given as $a = b = \omega = \nu = \gamma = \sigma = C = 0.5$. It is clearly seen that the solution (57) embodies the structure of dark soliton. The associated chirp is plotted in Fig. 13(c)-(d).

Case VI. Similarly, assuming that $A_0 = 0$, this leads to

$$\begin{aligned} H_1 &= -\frac{4A_1}{A_2}, \\ H_2 &= -\frac{8A_1}{A_2}, \\ H_3 &= 0, \\ s &= \sqrt{-A_1}, \end{aligned} \tag{59}$$

with the constraint conditions $16A_1A_3 = 3A_2^2$ given in terms of the physical parameters as

$$C = \frac{2(\lambda - 2\gamma)(3\lambda + 2\gamma)[2a\omega + (\nu + \sigma)^2] - 3[2ab - \lambda(\nu + \sigma)]^2}{2(\lambda^2 - 4\gamma^2)(3\lambda + 2\gamma)}. \tag{60}$$

By virtue of these results, one can find the exact optical soliton solution to Eq. (1) in the form

$$q(x,t) = \left\{ -\frac{4A_1}{A_2}\left[1 - \frac{2\mathrm{sech}^2\left(\sqrt{-A_1}\,\xi\right)}{4 - \left[1 - \tanh\left(\sqrt{-A_1}\,\xi\right)\right]^2}\right]\right\}^{\frac{1}{2}} e^{i(\phi(\xi) - \omega t)}, \tag{61}$$

which demands $A_1 < 0$ and $A_2 > 0$. Hence, the chirping is found as

$$\delta\omega(x,t) = -\frac{(\nu + \sigma)}{2a} - \frac{(3\lambda + 2\gamma)A_1}{aA_2}\left[1 - \frac{2\mathrm{sech}^2\left(\sqrt{-A_1}\,\xi\right)}{4 - \left[1 - \tanh\left(\sqrt{-A_1}\,\xi\right)\right]^2}\right] - \frac{CA_2}{4aA_1\left[1 - \frac{2\mathrm{sech}^2\left(\sqrt{-A_1}\,\xi\right)}{4 - \left[1 - \tanh\left(\sqrt{-A_1}\,\xi\right)\right]^2}\right]}. \tag{62}$$

This solution represents kink type soliton. In the event that $H_1 = 0$, we obtain an exact optical soliton solution to Eq. (1) characterizing anti-kink soliton in the form

$$q(x,t) = \left\{ -\frac{8A_1}{A_2}\left[\frac{\mathrm{sech}^2\left(\sqrt{-A_1}\,\xi\right)}{4 - \left[1 - \tanh\left(\sqrt{-A_1}\,\xi\right)\right]^2}\right]\right\}^{\frac{1}{2}} e^{i(\phi(\xi) - \omega t)}, \tag{63}$$

where $A_1 < 0$ and $A_2 > 0$. Accordingly, the associated chirp is written as

$$\delta\omega(x,t) = -\frac{(\nu + \sigma)}{2a} - \frac{2(3\lambda + 2\gamma)A_1}{aA_2}\left[\frac{\mathrm{sech}^2\left(\sqrt{-A_1}\,\xi\right)}{4 - \left[1 - \tanh\left(\sqrt{-A_1}\,\xi\right)\right]^2}\right] - \frac{CA_2\left(4 - \left[1 - \tanh\left(\sqrt{-A_1}\,\xi\right)\right]^2\right)}{8aA_1\mathrm{sech}^2\left(\sqrt{-A_1}\,\xi\right)}. \tag{64}$$

Fig. 14 exhibits the variations of soliton solution (61) with parameter values $a = b = \omega = \sigma = 0.5, \nu = 1, \gamma = -0.3, \lambda = 0.1$. From this figure, it is obviously seen that this solution represents kink type soliton. The soliton solution (63) is displayed in Fig. 15 with the same values of parameters as in Fig. 14. Based on the shown plot, this solution illustrates soliton wave of anti-kink shape. The chirping profile for kink type soliton is presented in Fig. 14(c)-(d) while the corresponding chirping for anti-kink wave is given in Fig. 15(c)-(d).

In all solutions obtained above, the phase variable $\phi(\xi)$ can be obtained via substituting $V(\xi)$ derived in each solution into the expression (16).

In order to investigate the influence of intensity dependent phase, which depends on the integration constant C, the associated chirp for all obtained solutions is illustrated numerically. The role of constant C in the chirping is examined. We can clearly see the changes in the chirp profiles as given in Figs. 1–15(c,d). The chirping structures are obviously affected due to the presence and absence of constant C. In addition to this, one can observe from the chirping expression (17) that the implementation of condition $\lambda = -2\gamma/3$ together with $C = 0$ generates chirp-free soliton solutions for the model (1), i.e. the phase component is linear function and independent of intensity.

4. Modulation instability analysis

In various nonlinear phenomena, dispersion and nonlinear effects arises due to instability in the steady-state modulation. Hence, we will utilize herein the linear stability analysis technique to study modulation instability of the perturbed NLSE (1).

Consider that Eq. (1) has the perturbed steady-state solution in the form

$$q(x,t) = \left[\sqrt{P} + Q(x,t)\right]e^{i\Phi}, \quad \Phi = bPt, \tag{65}$$

where $Q \ll P, P$ is the normalized optical power and Φ is the phase component. The perturbation $Q(x,t)$ is investigated by means of linear stability analysis. Inserting Eq. (65) into Eq. (1) and linearizing, one can reach

$$i\frac{\partial Q}{\partial t}+a\frac{\partial^2 Q}{\partial x^2}+bP(Q+Q^*)-i\left[\left(\sigma-2\lambda P-\gamma P\right)\frac{\partial Q}{\partial x}-(\lambda+\gamma)P\frac{\partial Q^*}{\partial x}\right]=0, \tag{66}$$

where $*$ denotes the conjugate of the complex function $Q(x,t)$. Suppose the solution of Eq. (66) in the form

$$Q(x,t)=\alpha e^{i(\kappa x-\varpi t)}+\beta e^{-i(\kappa x-\varpi t)}, \tag{67}$$

where κ and ϖ are the normalized wave number and frequency of perturbation, respectively. Substituting ansatz (67) into Eq. (66), we obtain two equations in α and β upon separating the coefficients of $\exp\{i(\kappa x-\varpi t)\}$ and $\exp\{-i(\kappa x-\varpi t)\}$ defined as

$$\begin{aligned}&(\varpi+\sigma\kappa-a\kappa^2)\alpha-[(\gamma+2\lambda)\alpha+(\gamma+\lambda)\beta]P\kappa+(\alpha+\beta)bP=0,\\&(\varpi+\sigma\kappa+a\kappa^2)\beta-[(\gamma+2\lambda)\beta+(\gamma+\lambda)\alpha]P\kappa-(\alpha+\beta)bP=0.\end{aligned} \tag{68}$$

From Eq. (68) we find the coefficient matrix of α and β in the form

$$\begin{bmatrix}\varpi+bP-(2\lambda P+\gamma P-\sigma)\kappa-a\kappa^2 & (b-\lambda\kappa-\gamma\kappa)P\\ -(b+\lambda\kappa+\gamma\kappa)P & \varpi-bP-(2\lambda P+\gamma P-\sigma)\kappa+a\kappa^2\end{bmatrix}\begin{bmatrix}\alpha\\ \beta\end{bmatrix}=\begin{bmatrix}0\\0\end{bmatrix}. \tag{69}$$

To ensure nontrivial solution for the coefficient matrix, the determinant has to be vanish. Thus, expanding the determinant leads to the dispersion relation given by

$$a^2\kappa^4+\left[(-2\gamma\lambda-3\lambda^2)P^2+(-2ab+2\gamma\sigma+4\lambda\sigma)P-\sigma^2\right]\kappa^2+2[(\gamma+2\lambda)P-\sigma]\kappa\varpi-\varpi^2=0. \tag{70}$$

The solution of the dispersion relation (70) for ϖ is given by

$$\varpi=[(\gamma+2\lambda)P-\sigma]\kappa\pm\kappa\sqrt{a^2\kappa^2+(\gamma+\lambda)^2P^2-2abP}. \tag{71}$$

This expression diagnoses the steady-state stability that depends on the group velocity dispersion, nonlinear effect, self-steepening perturbation, nonlinear dispersion and wave number. If $a^2\kappa^2+(\gamma+\lambda)^2P^2-2abP\geqslant 0$, then ϖ is real for all values of wave number κ and hence the steady state is stable against small perturbations. In contrast, the steady-state solution tends to be unstable if $a^2\kappa^2+(\gamma+\lambda)^2P^2-2abP<0$, i.e. ϖ is imaginary and this means that the perturbation grows exponentially. Consequently, the condition for the existence of modulation instability is introduced as

$$a^2\kappa^2+(\gamma+\lambda)^2P^2<2abP. \tag{72}$$

Accordingly, the growth rate of modulation instability gain spectrum $g(\kappa)$ can be defined as

$$g(\kappa)=2\,\mathrm{Im}(\varpi)=2|\kappa|\sqrt{a^2\kappa^2+(\gamma+\lambda)^2P^2-2abP}. \tag{73}$$

Fig. 16 shows the regions of modulation instability gain spectrum of Eq. (1) with distinct values for the model parameters. Three sets of parameter values are selected with the relation $\lambda=2\gamma$ and fixed value of incidence power to be $P=0.5$. The gain is sensitive to the sign and strength of the group velocity dispersion and the nonlinear effect, where both of them should have the same sign to ensure the occurrence of the MI gain. From the graph shown in Fig. 16a we can see that increasing the nonlinear coefficient and decreasing the group velocity dispersion enhance the MI growth rates. The 3D plot in Fig. 16b displays the evolution of the gain spectrum as a function of a and k while the 3D plot in Fig. 16c demonstrates the appearance of the two gain peaks depending on the change of γ and k.

5. Outlook and discussion

The three forms of soliton ansatzes have been very efficient on deriving various soliton solutions. The main structure obtained by applying these ansatzes is called W-shaped soliton which is given by (22), (30), (38) and generated under specific conditions. It has been taken into account that the pulse width and amplitude are real values. Thus, the parameters comply with the conditions $A_2<0$ and $A_1^2-3A_0A_2>0$. After the propagation, the W-shaped soliton wave is subject to degeneration into bright or dark solitons due to some restrictions. Although the condition $A_1<0, 3A_0A_2<0$ maintains the evolution of W-shaped soliton pulse, it is found that this structure collapses to bright soliton once the limit $A_1^2\gg|3A_0A_2|$ takes place. Besides, if the constraint $A_1>0, 3A_0A_2<A_1^2\leq 4A_0A_2$ came to pass, then this leads to the occurrence of dark soliton which turns into W-shaped soliton in the limit $A_1^2>4A_0A_2$. We found that the limit $A_1<0, 3A_0A_2>0$ gives rise to a complex type solution which is not under the scope of this work. It can be obviously seen from Fig. 17 that the graph shows the transition of wave profile from W-shaped soliton to bright and dark solitons according to the conditions mentioned above. Fig. 17 (a), (b), (c) depict solutions (22), (30), (38), respectively.

As the parameter $A_0=0$, W-shaped and bright solitons are exclusively recovered, where the former is described by solutions (24), (32) and (40) while the latter is represented by solutions (26), (34) and (42). All these solutions that introduce both of structures, i.e. W-shaped and bright solitons, are similar to their counterparts given by Triki et al. [38]. Moreover, the W-shaped structure given in (24) have been detected by Roy et al. [41] in a model describing the dynamics of Bose–Einstein condensate. The ansatz solution method in terms of cnoidal function was applied to derive localized solitons as the modulus of cnoidal function approaches 1. The obtained W-type soliton was found to be stable under the Vakhitov-Kolokolov criterion.

Additionally, the third soliton ansatz given by (36) has resulted in several exact solutions for the model (1). These solutions have been obtained depending on different relations between model parameters and they describe various types of soliton structures. Among theses structures are bright, dark, kink-dark, kink and anti-kink solitons.

6. Conclusion

In this work, the perturbed nonlinear Schrödinger equation in nano optical fibers is investigated. The nonlinear influence is of Kerr law type. The traveling wave theory enables us to reduce the complexity of the model to an elliptic type equation possessing many exact solutions. By applying the ansatz soliton solution having three different functional forms, the W-shaped soliton has been derived via a specific relation between the self-steepening effect and the nonlinear dispersion. It is noticed that this type of soliton pulses degenerates to bright and dark solitons under certain conditions. Further to this, various forms of wave structures are retrieved such as bright, dark, kink-dark, kink and anti-kink solitons. The validity for the existence of all solutions are determined. In accordance with the linear stability analysis, the modulation instability of the perturbed NLSE is studied. The modulation instability gain is found. The results obtained here are entirely new in nano optical fibers. We expect that these outcomes can be exploited in the physical and experimental applications of nonlinear optics.

CRediT authorship contribution statement

K.S. Al-Ghafri: Conceptualization, Methodology, Investigation, Writing - original draft. **E.V. Krishnan:** Validation, Writing - review & editing. **Anjan Biswas:** Investigation, Writing - review & editing.

Declaration of Competing Interest

The authors declare that they have no known competing financial interests or personal relationships that could have appeared to influence the work reported in this paper.

References

[1] Agrawal Govind P. Nonlinear fiber optics: quantum electronics–principles and applications. New York: Academic Press; 1995.
[2] Kivshar Yuri S, Agrawal Govind P. Optical solitons: from fibers to photonic crystals. Academic press; 2003.
[3] Biswas Anjan, Konar Swapan. Introduction to non-Kerr law optical solitons. CRC Press; 2006.
[4] Weizhu Bao. The nonlinear Schrödinger equation and applications in Bose-Einstein condensation and plasma physics. Dynamics in Models of Coarsening, Coagulation, Condensation and Quantization"(IMS Lecture Notes Series, World Scientific), 9: 141–240; 2007.
[5] Tsitsas NL, Rompotis N, Kourakis I, Kevrekidis PG, Frantzeskakis DJ. Higher-order effects and ultrashort solitons in left-handed metamaterials. Phys Rev E 2009;79 (3):037601.
[6] Biswas Anjan, Milovic Daniela, Milic Dejan. Solitons in alpha-helix proteins by He's variational principle. Int J Biomath 2011;4(04):423–9.
[7] Radhakrishnan R, Kundu A, Lakshmanan M. Coupled nonlinear Schrödinger equations with cubic-quintic nonlinearity: integrability and soliton interaction in non-kerr media. Phys Rev E 1999;60(3):3314.
[8] Fokas AS. On a class of physically important integrable equations. Physica D 1995; 87(1–4):145–50.
[9] Kundu Anjan, Mukherjee Abhik, Naskar Tapan. Modelling rogue waves through exact dynamical lump soliton controlled by ocean currents. Proc R Soc A: Math, Phys Eng Sci 2014;470(2164):20130576.
[10] Yin Hui-Min, Tian Bo, Cong-Cong Hu, Zhao Xin-Chao. Chaotic motions for a perturbed nonlinear Schrödinger equation with the power-law nonlinearity in a nano optical fiber. Appl Math Lett 2019;93:139–46.
[11] Bouzida Amel, Triki Houria, Ullah Malik Zaka, Zhou Qin, Biswas Anjan, Belic Milivoj. Chirped optical solitons in nano optical fibers with dual-power law nonlinearity. Optik 2017;142:77–81.
[12] Biswas Anjan, Asma Mir, Alqahtani Rubayyi T. Optical soliton perturbation with kerr law nonlinearity by Adomian decomposition method. Optik 2018;168:253–70.
[13] Gao Wei, Ghanbari Behzad, Günerhan Hatira, Baskonus Haci Mehmet. Some mixed trigonometric complex soliton solutions to the perturbed nonlinear Schrödinger equation. Mod Phys Lett B 2020;34(03):2050034.
[14] Sulaiman Tukur Abdulkadir, Bulut Hasan, Baskonus Haci Mehmet. Optical solitons to the fractional perturbed NLSE in nano-fibers. Discrete Continuous Dyn Syst-S 2020;13(3):925.
[15] Nestor Savaïssou, Houwe Alphonse, Betchewe Gambo, Doka Serge Y, et al. A series of abundant new optical solitons to the conformable space-time fractional perturbed nonlinear Schrödinger equation. Phys Scr 2020;95(8):085108.
[16] Foroutan Mohammadreza, Manafian Jalil, Ranjbaran Arash. Solitons in optical metamaterials with anti-cubic law of nonlinearity by generalized G'/G-expansion method. Optik 2018;162:86–94.
[17] Foroutan Mohammadreza, Manafian Jalil, Zamanpour Isa. Soliton wave solutions in optical metamaterials with anti-cubic law of nonlinearity by ITEM. Optik 2018; 164:371–9.
[18] Biswas Anjan. Chirp-free bright optical solitons and conservation laws for complex Ginzburg-Landau equation with three nonlinear forms. Optik 2018;174:207–15.
[19] Ekici Mehmet, Sonmezoglu Abdullah, Zhou Qin, Moshokoa Seithuti P, Ullah Malik Zaka, Arnous Ahmed H, Biswas Anjan, Belic Milivoj. Analysis of optical solitons in nonlinear negative-indexed materials with anti-cubic nonlinearity. Opt Quant Electron 2018;50(2):75.
[20] Abdel Kader AH, Abdel Latif MS, Zhou Qin. Exact optical solitons in metamaterials with anti-cubic law of nonlinearity by Lie group method. Opt Quant Electron 2019; 51(1):30.
[21] Al-Ghafri KS, Krishnan EV, Biswas Anjan, Ekici Mehmet. Optical solitons having anti-cubic nonlinearity with a couple of exotic integration schemes. Optik 2018; 172:794–800.
[22] Al-Ghafri Khalil S. Soliton behaviours for the conformable space–time fractional complex Ginzburg-Landau equation in optical fibers. Symmetry 2020;12(2):219.
[23] Zhou Qin, Zhong Yi, Mirzazadeh Mohammad, Bhrawy Ali H, Zerrad Essaid, Biswas Anjan. Thirring combo-solitons with cubic nonlinearity and spatio-temporal dispersion. Waves in random and complex media 2016;26(2):204–10.
[24] Liu Xiaoyan, Triki Houria, Zhou Qin, Mirzazadeh Mohammad, Liu Wenjun, Biswas Anjan, Belic Milivoj. Generation and control of multiple solitons under the influence of parameters. Nonlinear Dyn 2019;95(1):143–50.
[25] Weitian Yu, Zhou Qin, Mirzazadeh Mohammad, Liu Wenjun, Biswas Anjan. Phase shift, amplification, oscillation and attenuation of solitons in nonlinear optics. J Adv Res 2019;15:69–76.
[26] Ekici Mehmet, Zhou Qin, Sonmezoglu Abdullah, Moshokoa Seithuti P, Ullah Malik Zaka, Biswas Anjan, Belic Milivoj. Solitons in magneto-optic waveguides by extended trial function scheme. Superlattices Microstruct 2017;107:197–218.
[27] Liu Xiaoyan, Triki Houria, Zhou Qin, Liu Wenjun, Biswas Anjan. Analytic study on interactions between periodic solitons with controllable parameters. Nonlinear Dyn 2018;94(1):703–9.
[28] Liu Wenjun, Zhang Yujia, Triki Houria, Mirzazadeh Mohammad, Ekici Mehmet, Zhou Qin, Biswas Anjan, Belic Milivoj. Interaction properties of solitonics in inhomogeneous optical fibers. Nonlinear Dyn 2019;95(1):557–63.
[29] Zhou Qin, Liu Lan, Zhang Huijuan, Wei Chun, Jun Lu, Hua Yu, Biswas Anjan. Analytical study of Thirring optical solitons with parabolic law nonlinearity and spatio-temporal dispersion. Eur Phys J Plus 2015;130(7):138.
[30] Zhou Qin, Zhu Qiuping, Biswas Anjan. Optical solitons in birefringent fibers with parabolic law nonlinearity. Optica Applicata 2014;44(3):399–409.
[31] Biswas Anjan. Quasi–monochromatic dynamics of optical solitons having quadratic–cubic nonlinearity. Phys Lett A 2020:126528.
[32] Biswas Anjan. Optical soliton cooling with polynomial law of nonlinear refractive index. J Opt 2020:1–4.
[33] Zhonghao Li Lu, Li Huiping Tian, Zhou Guosheng. New types of solitary wave solutions for the higher order nonlinear Schrödinger equation. Phys Rev Lett 2000; 84(18):4096.
[34] Zhao Li-Chen, Li Sheng-Chang, Ling Liming. Rational W-shaped solitons on a continuous-wave background in the Sasa-Satsuma equation. Phys Rev E 2014;89 (2):023210.
[35] Triki Houria, Zhou Qin, Moshokoa Seithuti P, Ullah Malik Zaka, Biswas Anjan, Belic Milivoj. Chirped W-shaped optical solitons of Chen-Lee-Liu equation. Optik 2018;155:208–12.
[36] González-Gaxiola O, Biswas Anjan. W-shaped optical solitons of Chen–Lee–Liu equation by Laplace-Adomian decomposition method. Opt Quant Electron 2018;50 (8):314.
[37] Bendahmane Issam, Triki Houria, Biswas Anjan, Alshomrani Ali Saleh, Zhou Qin, Moshokoa Seithuti P, Belic Milivoj. Bright, dark and W-shaped solitons with extended nonlinear Schrödinger's equation for odd and even higher-order terms. Superlattices Microstruct 2018;114:53–61.
[38] Triki Houria, Bensalem Chaouki, Biswas Anjan, Zhou Qin, Ekici Mehmet, Moshokoa Seithuti P, Belic Milivoj. W-shaped and bright optical solitons in negative indexed materials. Chaos Solitons Fractals 2019;123:101–7.
[39] Vyas Vivek M, Patel Pankaj, Panigrahi Prasanta K, Kumar Choragudi Nagaraja, Greiner W. Chirped chiral solitons in the nonlinear Schrödinger equation with self-steepening and self-frequency shift. Phys Rev A 2008;78(2):021803.
[40] Saini A, Vyas VM, Raju Thokala Soloman, Pandey SN, Panigrahi Prasanta K. Super and subluminal propagation in nonlinear Schrödinger equation model with self-steepening and self-frequency shift. J Nonlinear Opt Phys Mater 2015;24(03): 1550033.
[41] Utpal Roy B, Shah Kumar Abhinav, Panigrahi PK. Gapped solitons and periodic excitations in strongly coupled BECs. J Phys B: At Mol Opt Phys 2011;44(3): 035302.